

Washington University School of Medicine

Digital Commons@Becker

Open Access Publications

6-1-2020

In vivo evolution of biopsy-proven inflammatory demyelination quantified by R2t* mapping

Biao Xiang

Jie Wen

Hsiang-Chih Lu

Robert E Schmidt

Dmitriy A Yablonskiy

See next page for additional authors


Follow this and additional works at: https://digitalcommons.wustl.edu/open_access_pubs

Authors

Biao Xiang, Jie Wen, Hsiang-Chih Lu, Robert E Schmidt, Dmitriy A Yablonskiy, and Anne H Cross

CASE STUDY

In vivo evolution of biopsy-proven inflammatory demyelination quantified by $R2t^*$ mapping

Biao Xiang¹, Jie Wen¹, Hsiang-Chih Lu², Robert E. Schmidt², Dmitriy A. Yablonskiy¹ & Anne H. Cross³ ¹Department of Radiology, Washington University, St. Louis, Missouri, 63110²Department of Pathology & Immunology, Washington University, St. Louis, Missouri, 63110³Department of Neurology, Washington University, St. Louis, Missouri, 63110

Correspondence

Anne H. Cross, Department of Neurology, Washington University, 660 South Euclid, Campus Box 8111, St. Louis, MO 63110, USA. Tel: +1(314)362-3293; Fax: +1(314) 747-1345; E-mail: crossa@neuro.wustl.edu

Funding Information

These studies were funded by a grant from the Conrad N. Hilton Foundation to Drs. Cross and Yablonskiy. Dr. Xiang is a Fellow of the National MS Society USA.

Received: 8 January 2020; Revised: 22 March 2020; Accepted: 10 April 2020

Annals of Clinical and Translational Neurology 2020; 7(6): 1055–1060

doi: 10.1002/acn3.51052

Introduction

The pathology of multiple sclerosis (MS) is heterogeneous, encompassing varying degrees of demyelination, inflammation, and axonal injury in both white and gray matter (WM/GM).¹ Standard clinical MRI does not correlate well with MS clinical disability,^{2,3} partly because it cannot discern the severities of these pathologies, and cannot detect abnormalities due to MS that are not sufficiently large or conspicuous. Moreover, areas that appear normal are often abnormal by histopathology; these regions are known as “normal-appearing” WM and GM (NAWM/NAGM). Thus, improved imaging biomarkers of MS tissue damage and repair are needed to better understand the evolution of MS pathology, and to facilitate the search for effective treatments. While different MRI-based methods have been proposed over the years for evaluation of MS-related tissue damage, a consensus on their application in clinical practice is still a work in progress.⁴

Abstract

A 35-year-old man with an enhancing tumefactive brain lesion underwent biopsy, revealing inflammatory demyelination. We used quantitative Gradient-Recalled-Echo (qGRE) MRI to visualize and measure tissue damage in the lesion. Two weeks after biopsy, qGRE showed significant $R2t^*$ reduction in the left optic radiation and surrounding tissue, consistent with the histopathological and clinical findings. qGRE was repeated 6 and 14 months later, demonstrating partially recovered optic radiation $R2t^*$, in concert with improvement of the hemianopia to ultimately involve only the lower right visual quadrant. These results support qGRE metrics as *in vivo* biomarkers for tissue damage and longitudinal monitoring of demyelinating disease.

We have previously proposed gradient echo imaging to measure $T2^*$ ($1/R2^*$) of brain tissue as an *in vivo* biomarker for quantitative evaluation of tissue damage in MS.⁵ Our measurements demonstrated significant $R2^*$ reductions in patients with MS. This result is in agreement with prior $R2$ ($1/T2$) measurements which correlated with white matter damage.⁶ To better understand the meaning of $R2^*$ reductions in MS-affected tissue, in this report we use recently developed quantitative gradient recalled echo (qGRE) MRI in a biopsied inflammatory demyelinating brain lesion.⁷ The qGRE method separates the tissue-cellular-specific $R2t^*$ from the total GRE signal decay $R2^*$, as total $R2^*$ can be altered by macroscopic field inhomogeneities and blood oxygen level-dependent effect (BOLD), affected by fluctuating physiological activity. Therefore, $R2t^*$ reflects tissue conditions more specifically than $R2^*$ in both white and gray matter of central nervous system (CNS). Our previous studies revealed a quantitative relationship between $R2t^*$ and normal

cortical neuronal density defined based on genetic information from the Allen Human Brain Atlas.⁸ We also reported reduced $R2t^*$ in MS NAGM, NAWM, and in WM MS lesions, finding that the extent of $R2t^*$ reductions correlated with the severity of upper extremity dysfunction and cognitive test scores.⁹

Herein, we demonstrate relationships of qGRE measurements with neuropathology findings in a person with a large parieto-occipital lesion who underwent biopsy and was found to have inflammatory demyelination. Furthermore, we show the evolution of the qGRE metrics over a period of 14 months correlated with the clinical evolution.

Methods

The Institutional Review Board of Washington University approved the MRI protocol. A 35-year-old right-handed man presented with right homonymous hemianopia and aphasia. MRI demonstrated a large left contrast-enhancing parieto-occipital lesion with mass effect on the posterior horn of the left lateral ventricle, along with two smaller nonspecific subcortical T2-weighted hyperintensities in the left frontal lobe. Spinal cord MRI was negative. Cerebrospinal fluid (CSF) studies revealed 29 nucleated cells (89% lymphocytes, 11% monocytes) and 6 CSF-restricted oligoclonal bands with normal IgG index (0.59). Comprehensive blood evaluations for infectious, rheumatologic, metabolic, and autoimmune disorders, including NMO-IgG, anti-MOG, and HIV tests, were negative. He was empirically treated with intravenous methylprednisolone followed by oral corticosteroids. Yet, repeat MRI 1 month later showed the lesion to be larger with extensive heterogeneous enhancement and greater mass effect. Because of the atypical course and worsening MRI, brain biopsy was performed 8 weeks after clinical onset. For tissue evaluation, histopathologic and immunohistochemical stains included Luxol fast blue–periodic acid Schiff (LFB-PAS; myelin), antibodies to neurofilament protein (axons), CD3 (T cells), CD163 (monocyte/macrophage, activated microglia), glial fibrillary acidic protein (GFAP) (activated astrocytes), and Prussian Blue (iron).

qGRE MRI scan was performed at 2 weeks, 6 months and 14 months after the biopsy using a 3T Prisma MRI

(Siemens, Germany). qGRE data were acquired using three-dimensional multigradient echo sequence with flip angle 30° , TR = 50 ms, voxel size $1 \times 1 \times 2 \text{ mm}^3$ and acquisition time 12 min. Ten gradient echoes, with first echo time TE1 = 4 ms and echo spacing $\Delta\text{TE} = 4 \text{ ms}$ were collected. In addition, Fluid-attenuated inversion recovery (FLAIR) images (voxel size $1 \times 1 \times 3 \text{ mm}^3$) and magnetization-prepared rapid gradient echo (MPRAGE) (voxel size $1 \times 1 \times 1 \text{ mm}^3$) were acquired.

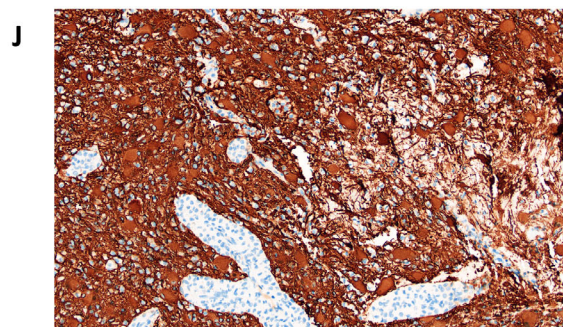
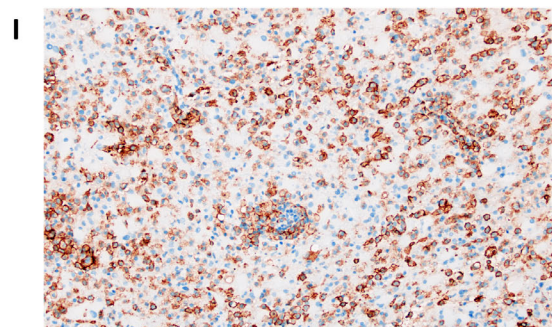
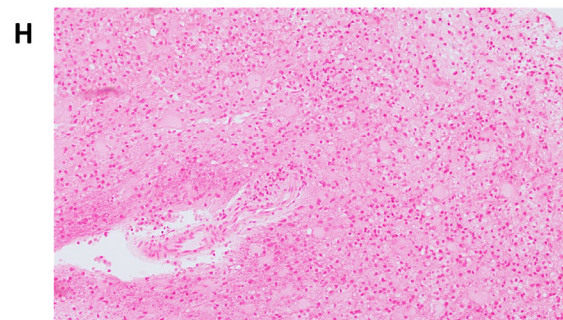
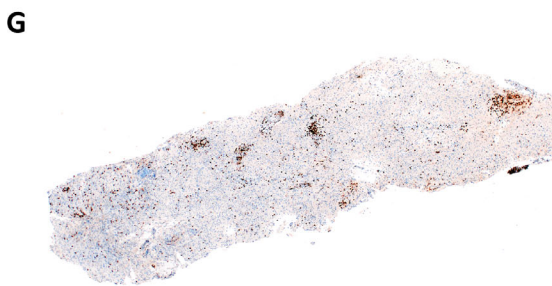
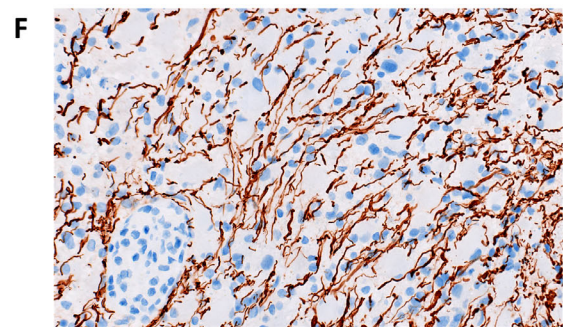
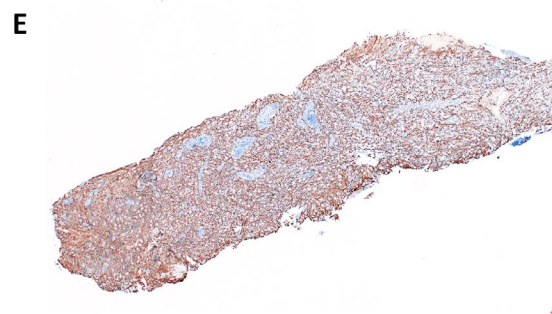
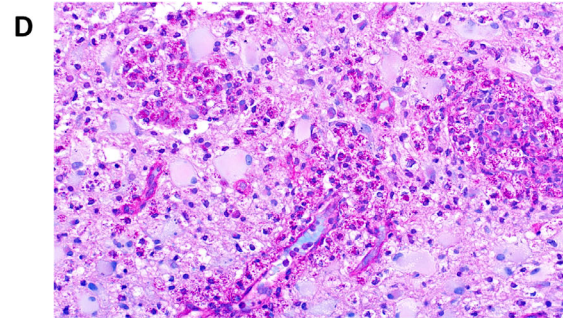
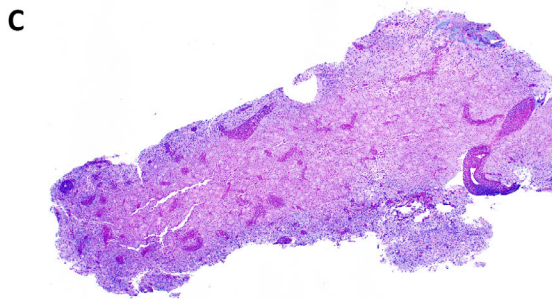
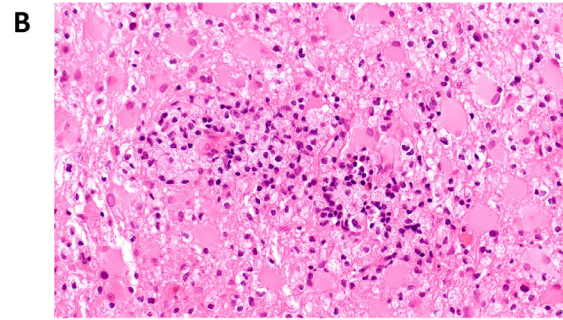
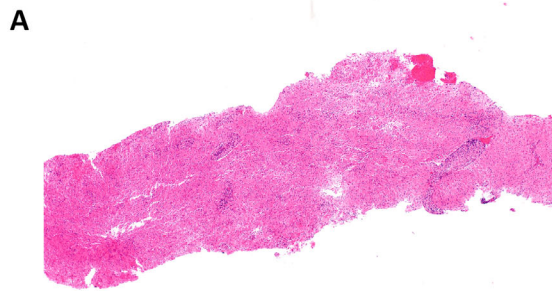
Quantitative $R2t^*$ images were generated using previously described methods.⁸ For each visit, MPRAGE and FLAIR images were registered using FSL 5.0.0 software (Analysis Group, FMRIB, Oxford, UK)¹⁰ and employed to obtain WM lesion masks using the “lesion-TOADS” tool¹¹ in Medical Image Processing, Analysis and Visualization (MIPAV).¹² The tissue damage score (TDS) for each voxel in the lesions was calculated as follows:

$$\text{TDS} = \frac{R2t^*_{\text{control}} - R2t^*_{\text{lesion}}}{R2t^*_{\text{control}} - R2t^*_{\text{CSF}}} \quad (1)$$

where $R2t^*_{\text{CSF}}$ is the $R2t^*$ value in the CSF (near zero), $R2t^*_{\text{lesion}}$ are the $R2t^*$ values in the lesion’s voxels, and $R2t^*_{\text{control}}$ is the “normal reference” $R2t^*$ value. For the latter, we collected qGRE data on three age- and gender-matched healthy control subjects. The median value of $R2t^*$ in the total white matter of the three healthy age- and gender-matched control subjects was computed (20.1 s^{-1}) and used as the “control reference.” Since inflammatory demyelination damages tissue, it leads to decreased $R2t^*$. Consequently, the TDS in the lesion is positive, approaching 1 in completely destroyed tissue void of macromolecules, similar to CSF. The mean TDS in the parietal-occipital lesion was calculated by averaging TDS in each voxel with exclusion of the biopsy needle path. In this study, the large parieto-occipital lesion was analyzed separately from the two small lesions in the left frontal lobe.

To better visualize the contribution of the optical radiation to $R2t^*$ signal, we used a two-compartment model in which the free water contribution within $R2t^*$ (set to 1 s^{-1} same as CSF) was filtered out, with the remainder, which we have termed $R2c^*$ relaxation, closely

Figure 1. Biopsied parieto-occipital lesion in left hemisphere revealed inflammatory demyelination. (A): Image of a hematoxylin and eosin (H&E, 4x magnification) stained biopsy specimen shows central regions of patchy pallor of the white matter, with an edge of normal white matter (at left lower edge) and perivascular mononuclear cell cuffing which is better visualized at higher magnification (20x) in (B). (C): An adjacent section stained with Luxol fast blue–periodic acid Schiff (LFB-PAS, 4x magnification) shows loss of myelin (loss of deep purple color). (D): Higher magnification (LFB-PAS, 20x) of the central demyelinated area shows little remaining myelin and macrophages with engulfed debris. (E): An adjacent section immunostained for neurofilaments (4x magnification) demonstrates relative sparing of axons in the area lacking myelin. (F): Higher magnification of (E) shows mainly normal-appearing axons (brown stain). (G): An adjacent section immunostained for CD3 reveals numerous perivascular CD3+ T cells (brown stain). (H): Prussian Blue staining (20x) for iron accumulation was negative. (I) CD163 staining for monocytes and activated microglia reveals numerous positive cells. (J) Glial fibrillary acidic protein (GFAP) staining shows activated astrocytes with reactive cytoplasm (gemistocytes) and numerous processes.



representing the contribution of cells and cellular processes. This approach is similar to free water mapping using diffusion MRI.¹³

Results

Microscopic images of the biopsied lesion (Fig. 1) showed regions of increased mononuclear cells, many of which were CD3+ T cells, along with highly reduced LFB-PAS stain indicating extensive demyelination. Relative preservation of neurofilament immunostaining (axons) was seen. This staining constellation indicated an inflammatory demyelinating process with relative axonal preservation. Axonal density was not measured as it was confounded by numerous intercalated macrophages and gliosis. Prussian Blue staining showed no iron accumulation within the biopsy (Fig. 1H). GFAP-positive activated astrocytes with numerous processes were present (Fig. 1J).

Five months postbiopsy, speech and language function had returned almost to normal, but the dense right homonymous hemianopia persisted. A clinical MRI at that time showed the left parieto-occipital lesion still present, but without Gd enhancement, with reduced mass effect and smaller FLAIR contrast size. Ten months postbiopsy, the patient was started on dimethyl fumarate for presumed MS. Fourteen months postbiopsy, clinical

examination revealed normal speech except for rare word-finding difficulty and only an inferior right quadrantanopia. Clinical FLAIR images show the tumefactive as well as two nonspecific lesions (Figure S1A).

qGRE measurements at 2 weeks, 6 months, and 14 months after biopsy revealed the left parieto-occipital lesion with reduced $R2t^*$, compared with surrounding tissue and the contralateral NAWM (Fig. 2C,H,L). This reduction was quantitatively characterized by TDS (Fig. 2D,I,M), with higher TDS values indicating worse tissue disruption. Over the 14 months, a substantial decrease in the lesion size and mean TDS, as well as the heterogeneity of the damage within the lesion, were observed. At the same time, the $R2t^*$ value in the contralateral side of the biopsied lesion remained stable across three visits (Figure S2A). The volume and the mean TDS of the other two small lesions (combined) over the three visits were 258 mm³ and 0.29, 128 mm³ and 0.28, 104 mm³ and 0.28, indicating progressive lesion size reduction.

$R2c^*$ images revealed a normal bright right optic radiation (red arrows in Fig. 2F,J,N). At visit 1, contrast between left optic radiation and surrounding tissue was reduced compared with the right side (Fig. 2F). By visit 2 and 3 the left optic radiation was becoming more visible.

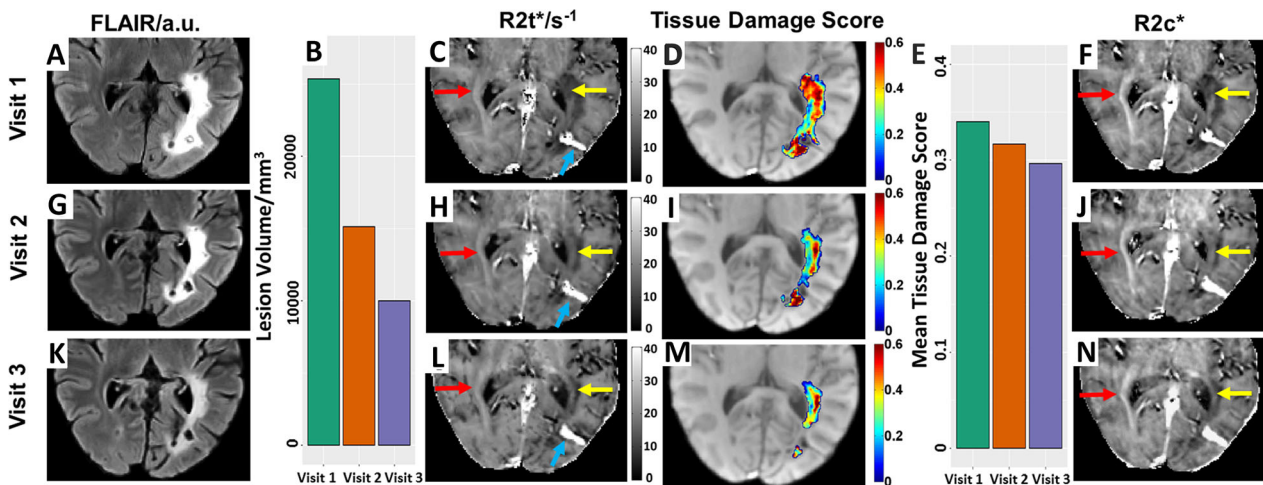


Figure 2. qGRE analyses of biopsied left parieto-occipital lesion. MRI data of visit 1, visit 2, and visit 3 were collected 2 weeks, 6 months, and 14 months after biopsy, respectively. The patient was started on dimethyl fumarate 10 months after biopsy. MRI images in visit 2 and 3 were registered to MRI images in visit 1. (A), (G), (K): FLAIR images showed the progressively reduced size of the left parieto-occipital lesion at visit 2 after 6 months and visit 3 after 14 months. (B). Lesion volume of the biopsied left parieto-occipital lesion decreased over the three visits. (C), (H), (L): $R2t^*$ images showed damaged optic radiation in the left hemisphere (yellow arrows vs. red arrows pointed to the intact right optic radiation) and bright biopsy needle path due to microhemorrhage (blue arrows). (D), (I), (M): Tissue damage score (TDS) calculated and color coded based on $R2t^*$ has been superimposed on the qGRE-T1w images. TDS map shows the heterogeneity of damage in the lesion. Higher TDS represents lower $R2t^*$, consistent with more severe tissue damage and/or greater edema. (E): Mean TDS in the left parieto-occipital lesion at three visits. Decreasing mean TDS in the lesion suggests improving tissue integrity over the 14 months. (F), (J), (N): $R2c^*$ images generated by filtering out free water contribution to $R2t^*$, allowing better visualization of optic radiation damage (arrows are the same as in $R2t^*$ images).

Discussion

We previously demonstrated that the qGRE $R2t^*$ metric⁷ can be used for *in vivo* evaluation of cortical neuronal density in healthy brain.⁸ In accord, reduction in cortical $R2t^*$ was significantly correlated with cognitive impairment in patients with both MS and Alzheimer Disease,^{9,14} suggesting that the amount and degree of cortical GM tissue damage can be estimated via voxel-wise $R2t^*$. We have also demonstrated that reductions in cortical $R2t^*$ are more sensitive to clinical dysfunction than are reductions in cortical thickness in patients with MS.⁹

Here, we have examined associations of brain biopsy results with qGRE-derived $R2t^*$ and $R2c^*$ metrics (the latter used to highlight WM tracts) in a man with inflammatory CNS demyelination with relative axonal sparing who was eventually diagnosed with MS. The biopsied lesion was active, given the histological presence of numerous macrophages and T cells around vessels and in CNS parenchyma, along with contrast enhancement on clinical MRI. The two smaller nonspecific lesions were not biopsied, but in retrospect are presumed to also be demyelinating lesions in this young man without comorbidities that might invoke other etiologies.

We also correlated qGRE metrics with clinical evolution on three visits spanning more than a year. At the first scan, high mean TDS in the parieto-occipital lesion corresponded with severe speech, language and visual deficits. By the third scan, substantially lower mean TDS was observed, in agreement with the progressive clinical improvement in speech, language, and visual function. The $R2t^*$ measurement in WM is affected by all tissue/cellular constituents, that is, lipids, proteins, iron etc. Consequently, loss of any of these components will lead to $R2t^*$ reduction, as seen in the lesion.

Since $R2c^*$ highlights myelinated fiber tracts by filtering out contributions of free water, it was applied to evaluate tissue damage in the left optic radiation apart from edema. On the initial scan, reduced $R2c^*$ suggested demyelination of the left optic radiation, consistent with the patient's right homonymous hemianopia. Although edema reduces $R2t^*$, the reduced $R2c^*$ indicated that pathology more than just edema was present, in agreement with histopathological results. At the second and third qGRE scans, $R2c^*$ contrast was more apparent in the left optic radiation, in concert with the progressive improvement of his right homonymous hemianopia to become an inferior right quadrantanopia. Hypothetically, the increase in both, $R2c^*$ and $R2t^*$ might indicate remyelination.

This study has a few limitations. The histopathological data were only acquired at the beginning of the qGRE study. Without serial histopathological data, we were

unable to directly confirm myelin loss, remyelination, and other disease related processes at later time-points. Also, the histopathology from a small biopsied area might not represent the pathology of the whole lesion. We followed the patient for only 14 months, whereas lesion evolution may be continuing for longer. Although the two-compartment model to provide $R2c^*$ relaxation achieves greater specificity by filtering out free water within $R2t^*$, $R2c^*$ has lower numerical accuracy compared with $R2t^*$, due to additional fitting parameters in the two-compartment model. Thus, we used $R2t^*$ rather than $R2c^*$ for TDS calculation.

In summary, we demonstrated *in vivo* sensitivity of the qGRE MRI to histopathology-verified inflammatory demyelination in a person who ultimately turned out to have MS. Compared with the standard FLAIR images, qGRE not only identified the lesion but also quantified the heterogeneous tissue damage within the lesion by TDS, and directly visualized WM tracts by $R2c^*$. Together, these results support qGRE metrics as potential quantitative and qualitative *in vivo* biomarkers for CNS demyelination and tissue damage.

Acknowledgment

The authors thank Dr. Emily Evans for referral of the patient for the study, Dr. John Ciotti for acquiring clinical images and Bryan Bollman for excellent technical assistance. These studies were funded by a grant from the Conrad N. Hilton Foundation to Drs. Cross and Yablonskiy. Dr. Xiang is a Fellow of the National MS Society USA.

Conflict of Interest

Dr. Anne Cross reports personal fees from Biogen, Celgene, EMD Serono, Genentech, Novartis, and TG Therapeutics, and grants from EMD Serono and from Genentech/Roche, outside the submitted work. Other authors have no competing interests, financial or otherwise.

Author Contributions

A.H.C., D.A.Y., and B.X. designed the study, supervised the experiments, and wrote the manuscript. A.H.C., D.A.Y., B.X., J.W., H.-C. L., and R.E.S. performed the experimental work and/or its analysis, and refined the manuscript.

References

1. Filippi M, Bar-Or A, Piehl F, et al. Multiple sclerosis. *Nature Reviews Disease Primers*. 2018;4:43.

2. Jakimovski D, Ramasamy DP, Zivadinov R. Magnetic Resonance Imaging and Analysis in Multiple Sclerosis. In: SA Rizvi, JF Cahill, PK Coyle, eds. *Clinical Neuroimmunology: Multiple Sclerosis and Related Disorders* pp. 109–136. Cham: Springer International Publishing, 2020.
3. McFarland HF, Barkhof F, Antel J, Miller DH. The role of MRI as a surrogate outcome measure in multiple sclerosis. *Multiple Sclerosis Journal*. 2002;8(1):40–51.
4. Oh J, Ontaneda D, Azevedo C, et al. Imaging outcome measures of neuroprotection and repair in MS: a consensus statement from NAIMS. *Neurology* 2019;92:519–533.
5. Sati P, Cross AH, Luo J, et al. In vivo quantitative evaluation of brain tissue damage in multiple sclerosis using gradient echo plural contrast imaging technique. *NeuroImage* 2010;51:1089–1097.
6. Laule C, Vavasour IM, Mädler B, et al. MR evidence of long T2 water in pathological white matter. *J Magn Reson Imaging* 2007;26:1117–1121.
7. Ulrich X, Yablonskiy DA. Separation of cellular and BOLD contributions to T2* signal relaxation. *Magn Reson Med* 2016;75:606–615.
8. Wen J, Goyal MS, Astafiev SV, et al. Genetically defined cellular correlates of the baseline brain MRI signal. *Proc Natl Acad Sci* 2018;115:E9727–E9736.
9. Xiang B, Wen J, Cross AH, Yablonskiy DA. Single scan quantitative gradient recalled echo MRI for evaluation of tissue damage in lesions and normal appearing gray and white matter in multiple sclerosis. *J Magn Reson Imaging* 2019;49:487–498.
10. Jenkinson M, Beckmann CF, Behrens TEJ, et al. *NeuroImage* 2012;62:782–790.
11. Shiee N, Bazin PL, Ozturk A, et al. A topology-preserving approach to the segmentation of brain images with multiple sclerosis lesions. *NeuroImage* 2010;49:1524–1535.
12. McAuliffe MJ, Lalonde FM, McGarry D, et al. editors. *Medical Image Processing, Analysis and Visualization in clinical research*. Proceedings 14th IEEE Symposium on Computer-Based Medical Systems CBMS 2001; 2001 26–27 July 2001.
13. Pasternak O, Sochen N, Gur Y, et al. Free water elimination and mapping from diffusion MRI. *Magn Reson Med* 2009;62:717–730.
14. Zhao Y, Raichle ME, Wen J, et al. In vivo detection of microstructural correlates of brain pathology in preclinical and early Alzheimer Disease with magnetic resonance imaging. *NeuroImage* 2017;148:296–304.

Supporting Information

Additional supporting information may be found online in the Supporting Information section at the end of the article.

Figure S1. Clinical FLAIR images show the large biopsied lesion and two small lesions in the left frontal lobe. (a), (b), (c) correspond to disease onset. (d), (e), (f) correspond to 1 month after disease onset. (g), (h), (i) correspond to 5 months after biopsy. Red arrows point at the small lesions in the left frontal lobe.

Figure S2. The $R2t^*$ values in the contralateral side of the biopsied lesion. A region of interest similar in size to the lesion that was biopsied was placed in the contralateral side. The $R2t^*$ values were measured in the same region for each visit. Results for $R2t^*$ values in the contralateral side were close to the normal healthy control value (20.1 s^{-1}) and showed little variation across the three visits. At the same time, $R2t^*$ in the lesion progressively decreased (up to 60%) (Fig. 2)